

Ba₂An(S₂)₂S₂ (An = U, Th): Syntheses, Structures, Optical, and Electronic Properties

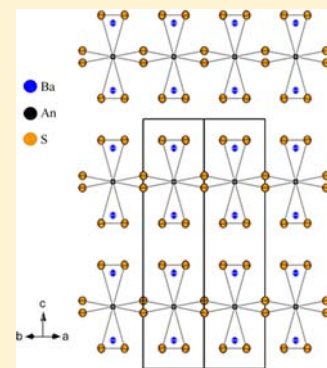
Adel Mesbah,[†] Emilie Ringe,[†] Sébastien Lebègue,[‡] Richard P. Van Duyne,[†] and James A. Ibers^{*,†}

[†]Department of Chemistry, Northwestern University, 2145 Sheridan Road, Evanston, Illinois 60208-3113, United States

[‡]Laboratoire de Cristallographie, Résonance Magnétique, et Modélisations CRM2 (UMR UHP-CNRS 7036), Faculté des Sciences et Techniques, Université de Lorraine, BP 70239, Boulevard des Aiguillettes, 54506 Vandoeuvre-lès-Nancy Cedex, France

Supporting Information

ABSTRACT: The compounds Ba₂An(S₂)₂S₂ (An = U, Th) have been synthesized by reactions of the elements with BaS and S at 1273 and 1173 K, respectively. These isostructural compounds crystallize in a new structure type in the tetragonal space group $D_{4h}^{15}-P4_2/nmc$. The structure comprises Ba²⁺ cations and $\infty[\text{An}(\text{S}_2)_2(\text{S})_2^{4-}]$ layers. The An⁴⁺ cations in these layers are arranged linearly and are bridged by S²⁻ anions. Coordination about the An center, which has symmetry $\bar{4}m2$, consists of two S₂²⁻ ions and four S²⁻ ions. Thus, the compounds are charge-balanced with An⁴⁺. No other alkali-metal actinide chalcogenides are known that contain chalcogen–chalcogen bonds. Optical measurements on Ba₂Th(S₂)₂S₂ indicate a direct band gap of 2.46(S) eV. Density functional theory calculations, performed with the HSE exchange–correlation potential, lead to band gaps of 2.2 and 1.8 eV for Ba₂Th(S₂)₂S₂ and Ba₂U(S₂)₂S₂, respectively, thus demonstrating the utility of applying this functional to 5f-electron systems.



INTRODUCTION

The crystal chemistry of the actinide chalcogenides An/Q (An = 5f element; Q = S, Se, or Te) has been widely explored. The presence of the 5f elements results in compounds that display varied structural, electronic, magnetic, and optical properties.^{1,2} These compounds are usually obtained by solid-state syntheses involving the reactive flux method³ or by direct combination of the elements.^{2,4}

Relatively few binary, ternary, and quaternary actinide chalcogenides exhibit Q–Q bonding (Q = S, Se, or Te). Among the sulfide binaries are US₃⁵ and An₂S₅ (An = Th, U).^{6–9} Among the ternaries that show Q–Q interactions are CsUTe₆,¹⁰ K₄USE₈,¹¹ and the relatively large family of AA₂Q₆ compounds (with A = K, Rb, or Cs; An = U, Th, or Np, Q = S, Se, or Te) whose structure types are CsTh₂Te₆¹² and KTh₂Se₆.¹³ The quaternaries RbSbU₂S₈¹⁴ and Ta₂UO(S₂)₃Cl₆¹⁵ display S–S bonds.

All but the last compound are binaries or are formed by the insertion of a monovalent cation to form a ternary or a quaternary. The insertion of an alkali-metal cation (Ak) to form a ternary or a quaternary (with further insertion of another cation) remains largely uninvestigated. In the Ak/An/Q family, the compounds BaUS₃,^{16,17} AkU₂S₅ (Ak = Ca, Sr, Ba),^{18,19} and SrTh₂Se₅⁴ are known. Several quaternaries (Ak/An/M/Q) are also known. These include Ba₂Cu₂US₅,²⁰ Ba₄Cr₂US₉,²⁰ and Ba₈Hg₃U₃S₁₈.²¹ None of these contain Q–Q bonds.

One objective of the present work was to explore the synthesis of actinide chalcogenides containing an alkaline-earth metal. The size and charge of an alkaline-earth metal, as opposed to those of an alkali metal, will surely lead to new compounds and structures. In the present work, the syntheses

and structure of the two new isostructural compounds Ba₂U(S₂)₂S₂ and Ba₂Th(S₂)₂S₂ are described. These differ from the other Ak/An/Q compounds in that they contain Q–Q single bonds. A second objective of the present study was to assess the utility of the HSE functional in density functional theory (DFT) calculations of band gaps in 5f-electron systems. We thus describe some optical properties of Ba₂Th(S₂)₂S₂ and the electronic properties of both compounds as calculated by the DFT method performed with the HSE exchange–correlation potential.

EXPERIMENTAL METHODS

Syntheses. The following reactants were used as starting materials: ²³⁸U powder, obtained by hydridization and decomposition of U turnings (ORNL) in a modification²² of a literature method,²³ Th powder (MP Biomedicals, LLC 99.1%), BaS (Alfa, 99.7%), and S (Mallinckrodt, 99.6%). The reactions were performed in sealed carbon-coated fused-silica tubes. The starting mixtures were loaded into such tubes under an Ar atmosphere in a glovebox. Then the tubes were evacuated to 10^{−4} Torr, flame-sealed, and placed in a computer-controlled furnace. The elemental composition was determined qualitatively with an energy-dispersive X-ray (EDX)-equipped Hitachi S-3400 scanning electron microscope.

Ba₂U(S₂)₂S₂. Very small black blocks of Ba₂U(S₂)₂S₂ in about 20 wt % yield based on U were obtained by the reaction of BaS (21.6 mg, 0.128 mmol), U (20.2 mg, 0.085 mmol), and S (9.5 mg, 0.298 mmol). The reaction mixture was heated to 1273 K in 48 h, held there for 4 h, cooled to 1223 K in 12 h, kept there for 8 days, and then cooled to 298 K at 3 K/h. EDX analysis performed on selected black blocks showed

Received: October 11, 2012

Published: November 29, 2012

Ba/U/S in the approximate ratio 2:1:6. The major product of the reaction was polycrystalline UOS.

Ba₂Th(S₂)₂S₂. This compound was synthesized from the mixture of BaS (28.8 mg, 0.17 mmol), Th (19.8 mg, 0.084 mmol), and S (16.35 mg, 0.51 mmol). This mixture was heated to 1173 K, kept there for 4 days, and then cooled to 473 K at 3 K/h, and then the furnace was turned off. Green plates in about 50 wt % yield based on Th were isolated and analyzed by EDX. These showed Ba/Th/S in the approximate ratio 2:1:6. The other product was ThOS, as judged by its color and the habit of the crystals, together with EDX analysis of Th:S = 1:1.

Structure Determinations. Single-crystal X-ray diffraction data for Ba₂U(S₂)₂S₂ and Ba₂Th(S₂)₂S₂ were collected with the use of graphite-monochromatized Mo K α radiation ($\lambda = 0.71073$ Å) at 100 K on a Bruker APEX2 diffractometer.²⁴ The data collection strategy was optimized with the algorithm COSMO in the program APEX2²⁴ as a series of 0.3° scans in ω and ϕ . The exposure time was 10 s/frame. The crystal-to-detector distance was 6 cm. The collection of the intensity data as well as cell refinement and data reduction was carried out with the use of the program APEX2.²⁴ Face-indexed absorption, incident beam, and decay corrections were performed with the use of the program SADABS.²⁵ Both structures were solved and refined with the use of the SHELXTL programs.²⁶ The program STRUCTURE TIDY²⁷ in PLATON²⁸ was used to standardize the atomic positions. Further details are given in Table 1 and in the Supporting Information.

Table 1. Crystal Data and Structure Refinements for Ba₂U(S₂)₂S₂ and Ba₂Th(S₂)₂S₂^a

	Ba ₂ U(S ₂) ₂ S ₂	Ba ₂ Th(S ₂) ₂ S ₂
fw (g mol ⁻¹)	705.07	699.08
color	black	green
<i>a</i> (Å)	5.4145(2)	5.4810(2)
<i>c</i> (Å)	15.7322(5)	15.9860(6)
<i>V</i> (Å ³)	461.22(3)	480.24(4)
ρ (g cm ⁻³)	5.077	4.834
μ (mm ⁻¹)	27.229	24.776
<i>R</i> (<i>F</i>) ^b	0.0144	0.0187
<i>R</i> _w (<i>F</i> _o ²) ^c	0.0346	0.0378

^aFor both structures, space group $D_{4h}^{15}P4_2/nmc$, $Z = 2$, $\lambda = 0.71073$ Å, and $T = 100(2)$ K. ^b $R(F) = \sum ||F_o| - |F_c|| / \sum |F_o|$ for $F_o^2 > 2\sigma(F_o^2)$. ^c $R_w(F_o^2) = \{ \sum [w(F_o^2 - F_c^2)]^2 / \sum w F_o^4 \}^{1/2}$. For $F_o^2 < 0$, $w^{-1} = \sigma^2(F_o^2)$; for $F_o^2 \geq 0$, $w^{-1} = \sigma^2(F_o^2) + (qF_o^2)^2$, where $q = 0.0106$ for Ba₂U(S₂)₂S₂ and 0.0183 for Ba₂Th(S₂)₂S₂.

Optical Measurements. Optical absorption measurements for Ba₂Th(S₂)₂S₂ were performed over the range from 3.76 eV (330 nm) to 1.39 eV (894 nm) at 293 K on four and six different regions along the (001) crystal faces of two distinct single crystals. Each was mounted on a goniometer head and inserted on a custom-made holder fitted to a Nikon Eclipse Ti2000-U inverted microscope.^{29,30} The crystal was positioned at the focal plane above the 20 \times objective of the microscope and illuminated with a tungsten–halogen lamp. The transmitted light was spatially filtered with a 200 μ m aperture, dispersed by a 150 grooves/mm grating in an Acton SP2300i imaging spectrometer, and collected on a back-illuminated, LN₂-cooled charge-coupled device (Spec10:400BR, Princeton Instruments). Polarization experiments were performed by inserting a polarizer between the lamp and crystal; spectra were taken at 10° increments of the polarizer angle.

Similar measurements on Ba₂U(S₂)₂S₂ were not possible because of the small size of the crystals and contamination of Ba₂U(S₂)₂S₂ powder by UOS.^{31,32}

Computational Calculations. The calculations were performed within the framework of DFT³³ together with the exchange–correlation potential HSE06.^{34–36} In this formulation, the exchange potential contains a part of the Hartree–Fock potential for the short-range part of the interaction, while the correlation potential is kept at the

generalized gradient approximation (GGA) level.³⁷ In particular, HSE06 is known to cure partly the problem of self-interaction and also to provide band gaps that usually are in reasonable agreement with the experiment.³⁸ Although the HSE functional is becoming increasingly popular, it has not been applied widely to systems containing *f* electrons, although one can cite, for example, works on UO₂, PuO₂, and Pu₂O₃³⁹ and on CeO₂ and Ce₂O₃,^{40–42} with satisfactory results in comparison to the available experiments *The Vienna ab Initio Simulation Package* (VASP)^{43,44} implementing the projector-augmented wave method⁴⁵ was used to perform the ab initio simulations. A 6 \times 6 \times 2 *k*-point mesh was used to sample the Brillouin zone together with the default cutoff for the plane-wave expansion. The lattice parameters and positions of the atoms were kept identical with those obtained experimentally. Spin polarization was allowed, and the two possible configurations (ferromagnetic or antiferromagnetic) within the crystal cell were checked. Also, the optical properties were calculated using the HSE eigenvalues and orbitals in the sum-over-states approximation, as implemented⁴⁶ in the VASP code.

DISCUSSION

Syntheses. The compounds Ba₂U(S₂)₂S₂ and Ba₂Th(S₂)₂S₂ were synthesized by the reactions of U or Th with BaS and S at 1273 and 1173 K, respectively. The yield of very small black blocks of Ba₂U(S₂)₂S₂ was about 20 wt % based on U, with the other product being UOS. No single crystals larger than about 40 μ m could be made. The yield of green plates of Ba₂Th(S₂)₂S₂ was approximately 50 wt % based on Th, with the other product being ThOS.³⁰ Because ThOS and UOS are very stable³⁰ and both Th and U are oxyphilic, attack on the silica tubes, even if the tubes were carbon-coated, presumably led to these byproducts. Repeated attempts to optimize yields failed. Attempts to synthesize the Se or Te analogues failed; only BaQ and UQ₂ resulted. A few Ak/U/Se compounds have been synthesized at 1423 K,¹⁹ which is beyond the temperature limit of our furnaces.

Structure. The isostructural compounds Ba₂U(S₂)₂S₂ and Ba₂Th(S₂)₂S₂ crystallize with two formula units in the tetragonal space group $D_{4h}^{15}P4_2/nmc$ in a new structure type in cells with $a = 5.4145(2)$ Å and $c = 15.7322(5)$ Å [Ba₂U(S₂)₂S₂] and $a = 5.4810(2)$ Å and $c = 15.9860(6)$ Å [Ba₂Th(S₂)₂S₂]. The asymmetric unit contains one An atom (site symmetry $\bar{4}m2$), one Ba atom ($2mm$), and two S atoms [S1 (m) and S2 ($2mm$)]. A general view of the structure approximately down [110] is presented in Figure 1. The structure consists of ${}^2_\infty[\text{An}(\text{S}_2)_2(\text{S}_2)_4^-]$ layers (Figure 2) and Ba²⁺ cations. The layers are stacked perpendicular to [001]. Each An center is coordinated to two S1–S1 pairs and four S2 atoms (Figure 3). Coordination may be described as pseudooctahedral if one considers the four S2 atoms and the centers of the two S1–S1 pairs. Metrical data are given in Table 2. The U–S distances are 2.8199(7) and 2.7337(2) Å for S1 and S2, respectively; the Th–S distances are 2.889(1) and 2.7759(3) Å. That the U–S distances are shorter than the corresponding Th–S distances is a manifestation of the actinide contraction. The U–S distances are typical for eight-coordinate U⁴⁺ and comparable to those observed in K_{0.92}U_{1.79}S₆, Rb_{0.85}U_{1.74}S₆, and RbSbU₂S₈ (Table 3). The Th–S distances are comparable to those of 2.844(2) and 2.968(1) Å for eight-coordinate Th⁴⁺ in K₁₀Th₃(P₂S₇)₄(PS₄)₂⁴⁷ and may be compared to those for six-coordinate Th⁴⁺ in KCuThS₃, K₂Cu₂ThS₄, and K₃Cu₃Th₂S₇.⁴⁸

In Ba₂U(S₂)₂S₂ and Ba₂Th(S₂)₂S₂, each Ba center (symmetry $2mm$) is surrounded by six S1 and two S2 atoms, with Ba–S distances ranging between 3.2167(6) and 3.2978(7) Å and

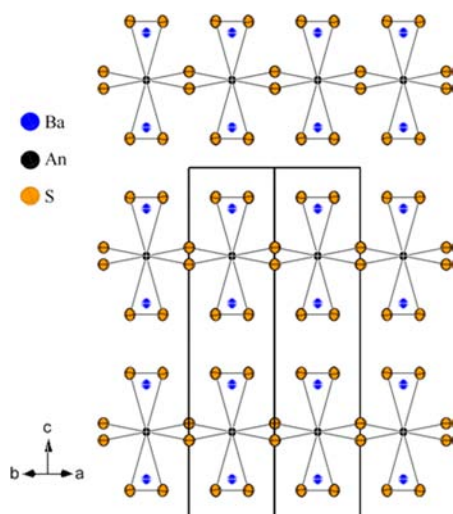


Figure 1. Structure of $\text{Ba}_2\text{An}(\text{S}_2)_2\text{S}_2$ (An = U, Th) approximately down the a axis.

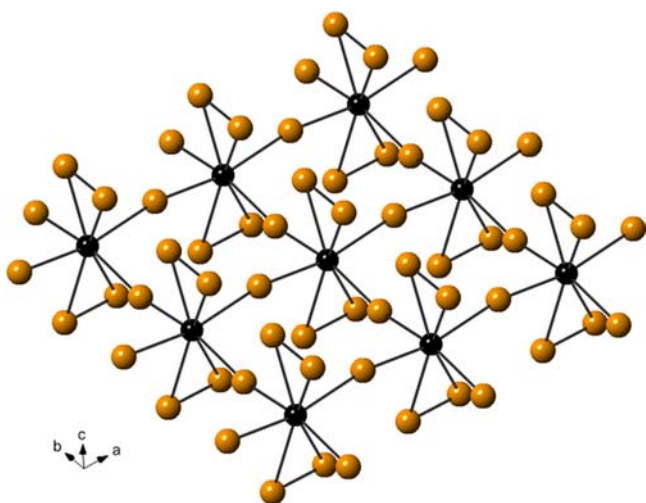


Figure 2. $2. [\text{An}(\text{S}_2)_2(\text{S})_2]^{4-}$ layer in $\text{Ba}_2\text{An}(\text{S}_2)_2\text{S}_2$ (An = U, Th).

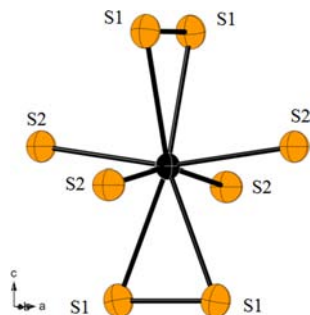


Figure 3. Local coordination of the An (U, Th) center in $\text{Ba}_2\text{An}(\text{S}_2)_2\text{S}_2$. Symmetry $4m2$ is imposed.

between 3.252(1) and 3.281(2) Å, respectively. These distances are comparable to the BaS_8 interatomic distances of 3.123(9) and 3.609(7) Å in BaUS_3 .¹⁷

The S1–S1 distances are 2.082(1) Å (U) and 2.098(2) Å (Th). Such distances are typical of a S–S single bond, for example, 2.055(2) Å in S_8 ;⁴⁹ hence the formulation of the compounds as $\text{Ba}_2\text{An}(\text{S}_2)_2\text{S}_2$.

Table 2. Selected Interatomic Distances (Å) for $\text{Ba}_2\text{U}(\text{S}_2)_2\text{S}_2$ and $\text{Ba}_2\text{Th}(\text{S}_2)_2\text{S}_2$ ^a

	$\text{Ba}_2\text{U}(\text{S}_2)_2\text{S}_2$	$\text{Ba}_2\text{Th}(\text{S}_2)_2\text{S}_2$
An–S1	$2.8199(7) \times 4$	$2.889(1) \times 4$
An–S2	$2.7337(2) \times 4$	$2.7759(3) \times 4$
S1–S1	2.082(1)	2.098(2)
Ba–S1	$3.2187(4) \times 4$	$3.2591(7) \times 4$
Ba–S1	$3.2978(7) \times 2$	$3.281(1) \times 2$
Ba–S2	$3.2167(6) \times 2$	$3.252(1) \times 2$

^aAtoms have the following site symmetries: An ($\bar{4}m2$), Ba (2 mm.), S1 (m.), S2 (2 mm.).

Table 3 lists the An/S compounds in which S–S single bonds are present. The new structure adopted by $\text{Ba}_2\text{U}(\text{S}_2)_2\text{S}_2$ and $\text{Ba}_2\text{Th}(\text{S}_2)_2\text{S}_2$ comprises Ba^{2+} cations and $2. [\text{An}(\text{S}_2)_2(\text{S})_2]^{4-}$ layers (Figure 1). The An^{4+} cations in these layers are arranged linearly and are bridged by S^{2-} anions (Figure 2). This arrangement of An^{4+} cations is markedly different from those found in the layers in US_3 ,⁵ $\text{K}_{0.92}\text{U}_{1.79}\text{S}_6$,⁵⁰ and $\text{Rb}_{0.85}\text{U}_{1.74}\text{S}_6$,⁵¹ these are based on the ZrSe_3 structure.⁵² In these structures, the layers are composed of double chains of An^{4+} cations (Figure 4). The layers in RbSbU_2S_8 ¹⁴ are composed of similar US_8 polyhedra. However, these share S atoms, with the Sb atoms situated in the centers of slightly distorted seesaws (Figure 4). In the structure of $\text{Ta}_2\text{UO}(\text{S}_2)_3\text{Cl}_6$,¹⁵ there are two different S–S bonds that are shared between U and Ta and a third S–S bond that is shared between Ta atoms. In the three-dimensional An_2S_5 structures, the S–S bonds are shared by four An centers.

Absorbance of $\text{Ba}_2\text{Th}(\text{S}_2)_2\text{S}_2$. A fundamental absorption edge is clearly visible in the transmission measurements (Figure 5). Extrapolation to the absorption edge shows that $\text{Ba}_2\text{Th}(\text{S}_2)_2\text{S}_2$ is a semiconductor. The direct and indirect band gaps derived from a total of 10 measurements on two different crystals are 2.46(5) and 2.42(6) eV, respectively; these are consistent with the light-green color of the crystals. A comparison of plots of absorbance versus energy ($h\nu$; Figure 5, top) to plots of $(ah\nu)^{1/2}$ (Figure 5, bottom left) and $(ah\nu)^2$ (Figure 5, bottom right) versus $h\nu$ indicates that the transition is direct. No polarization dependence was observed along the [001] direction of three different crystals when the polarization of visible light was scanned from 0 to 360°.

Theoretical Results. The computed total (DOS) and partial density of states (PDOS) are presented from –5 to +5 eV (the Fermi level is put at 0 eV) in Figures 6 and 7 for $\text{Ba}_2\text{Th}(\text{S}_2)_2\text{S}_2$ and $\text{Ba}_2\text{U}(\text{S}_2)_2\text{S}_2$, respectively. For each atom, an orbital-resolved PDOS is plotted. Within the different magnetic orders allowed in the crystallographic cell, $\text{Ba}_2\text{Th}(\text{S}_2)_2\text{S}_2$ is found to be nonmagnetic, whereas $\text{Ba}_2\text{U}(\text{S}_2)_2\text{S}_2$ is found to be antiferromagnetic but almost degenerate with the ferromagnetic solution in terms of total energy. Therefore, for $\text{Ba}_2\text{U}(\text{S}_2)_2\text{S}_2$ spin-polarized PDOS are presented.

From their total DOS, both compounds have sizable band gaps. In particular, $\text{Ba}_2\text{Th}(\text{S}_2)_2\text{S}_2$ (Figure 6) has a band gap of 2.2 eV, with the top of the valence band being derived mainly from S1 p states, whereas the bottom of the conduction band is composed mainly of Th d states. The states from –5 to 0 eV originate from S1 and S2, whereas the conduction bands up to 5 eV come from Ba d, Th d, and Th f states. The PDOS of S2 and Th share similar features at –0.6 and –2.8 eV, which indicates a significant bonding between these two species. The PDOS of Ba is more difficult to analyze because it exhibits low

Table 3. Actinide Compounds Containing S–S Single Bonds

	structure	An–S range (Å)	S–S distance	ref
Ba ₂ U(S ₂) ₂ S ₂	layered	2.7337(2)–2.8199(7)	2.082(1)	this work
Ba ₂ Th(S ₂) ₂ S ₂	layered	2.7759(3)–2.889(1)	2.098(2)	this work
US ₃	layered	2.753(2)–2.825(2)	2.086(4)	5
K _{0.92} U _{1.79} S ₆	layered	2.761(2)–2.846(2)	2.097(5)	50
Rb _{0.85} U _{1.74} S ₆	layered	2.775(3)–2.847(2)	2.106(5)	51
RbSbU ₂ S ₈	layered	2.752(3)–2.854(1)	2.096(5)	14
Ta ₂ UO(S ₂) ₃ Cl ₆	chains	2.819(3)–2.928(3)	2.081(4), 2.077(4)	15
U ₂ S ₅	three dimensional	2.801–3.089	2.072	8
Th ₂ S ₅	three dimensional	2.861(4)–3.163(4)	2.117(7)	6–9

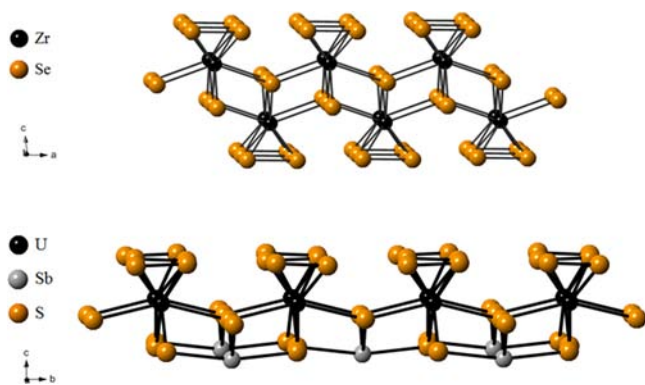


Figure 4. Arrangement of the cations in a layer of the ZrSe₃ structure⁵² (top) and the RbSbU₂S₈ structure¹⁴ (bottom).

values for a wide range of energies below the Fermi level; these can be affected by the details of the numerical procedure.

In contrast, Ba₂U(S₂)₂S₂ (Figure 7) has a band gap of 1.8 eV, with the top of the valence band made up of S2 p and U f

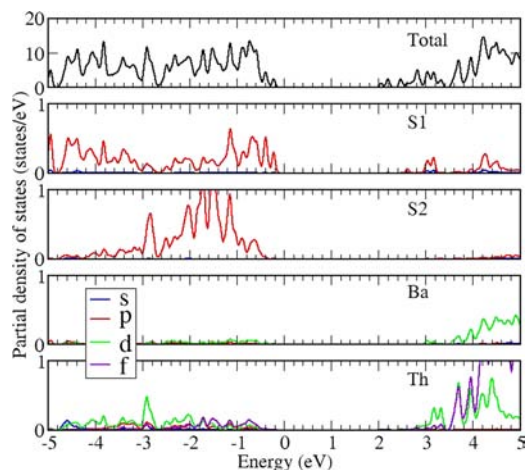


Figure 6. DOS (upper plot) and PDOS (lower plots) for Ba₂Th(S₂)₂S₂. For each atom, the PDOS is projected onto the relevant orbitals.

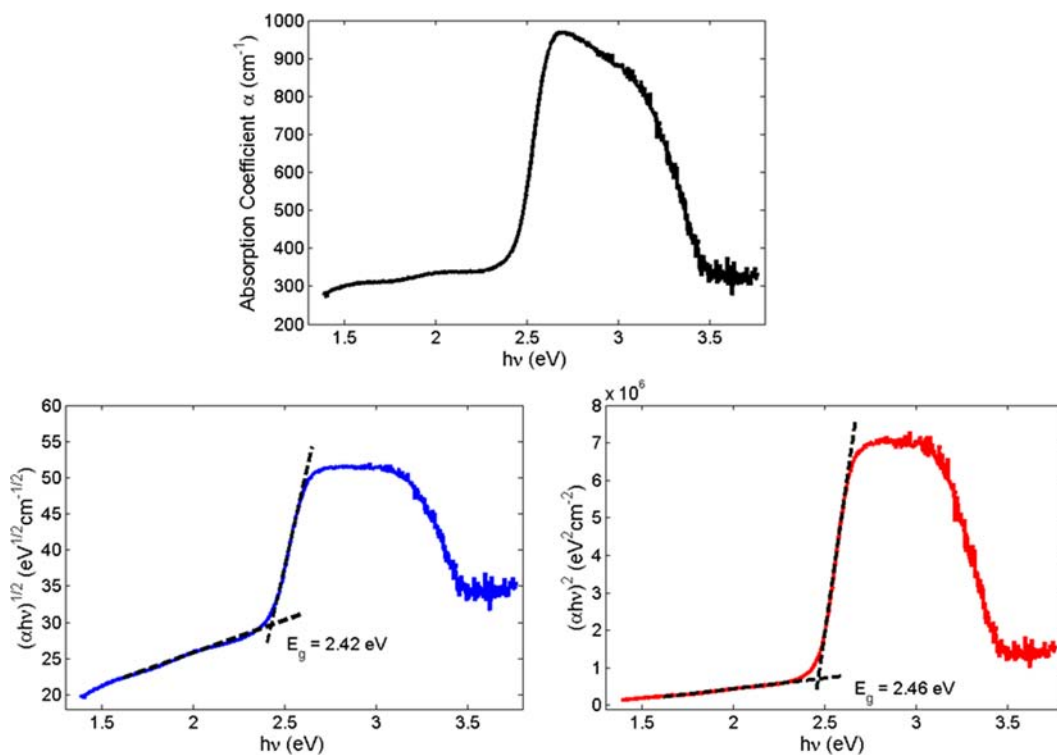


Figure 5. Absorbance of Ba₂Th(S₂)₂S₂. Top: absorbance (α) versus energy ($h\nu$). Bottom left: spectrum calculated for an indirect band gap. Bottom right: spectrum calculated for a direct band gap.

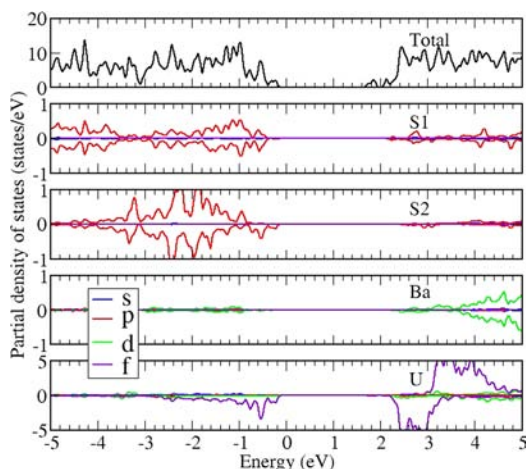


Figure 7. DOS (upper plot) and PDOS (lower plots) for $\text{Ba}_2\text{U}(\text{S}_2)_2\text{S}_2$. For each atom, the PDOS is projected onto the relevant orbitals.

states. The bottom of the conduction band is more difficult to identify from the different PDOS. Although a small contribution appears to come from the unoccupied U f states, most correspond to the contribution to the total DOS from the interstitial region not covered by the spheres around each atom that were used to obtain the PDOS. As for $\text{Ba}_2\text{Th}(\text{S}_2)_2\text{S}_2$, the states from -5 to 0 eV are derived from S1 and S2 states, but now for $\text{Ba}_2\text{U}(\text{S}_2)_2\text{S}_2$, the f-electron shell is partly filled and contributes to the total DOS for this range of energy. For the conduction bands up to 5 eV, all of the atoms are contributing. Also, the spin polarization of the U atom is clearly seen on the corresponding PDOS plot. It induces a spin polarization of the Ba and S2 atoms, whereas the S1 atoms seem to be less affected by the magnetic moment on the U atoms.

For a comparison with the optical measurements on $\text{Ba}_2\text{Th}(\text{S}_2)_2\text{S}_2$, we have calculated the imaginary part of the dielectric function for the two independent directions (ϵ_{xx} and ϵ_{zz}) in the crystal (Figure 8). Both ϵ_{xx} and ϵ_{zz} show

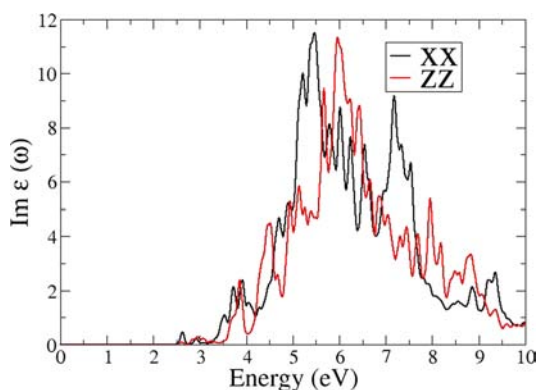


Figure 8. Calculated imaginary part of the dielectric function of $\text{Ba}_2\text{Th}(\text{S}_2)_2\text{S}_2$ for the two independent directions (ϵ_{xx} and ϵ_{zz}) in the crystal.

many peaks that correspond to the different direct transitions allowed between the valence and conduction bands. Also, the observed threshold for transitions is positioned at about 2.5 eV, although the precision is limited because we have used a smearing technique to achieve integration over the Brillouin zone. The band structure (Figure 9) shows that the minimum direct transitions occur around the high-symmetry points X and

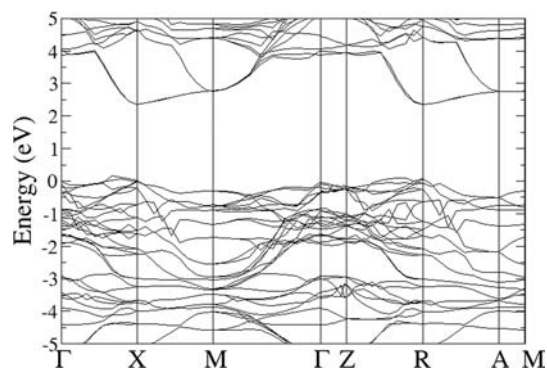


Figure 9. Calculated band structure for $\text{Ba}_2\text{Th}(\text{S}_2)_2\text{S}_2$ along some high-symmetry directions.

R. In particular, the value of the corresponding direct band gap is 2.4 eV, which is in good agreement with the threshold observed in the imaginary part of the dielectric function. The gap of 2.2 eV observed in the total DOS corresponds to the indirect minimum band gap between the valence states along the X–M and Z–R directions and the conduction states at the X and R high-symmetry points. Because we have used the HSE functional, as opposed to the usual functionals, such as the local density approximation or GGA, or even the GGA+U approximation, to treat this strongly correlated system, our theoretical band gap is found to be in reasonable agreement³⁸ with the experimental value.

A quantitative understanding of the electron distribution in the crystal can be achieved with the use of Bader's analysis.⁵³ In order to carry out this analysis, the charge density in real space must be reconstructed properly from the projector-augmented wave basis set.⁵⁴ Applying Bader's analysis to our computed electron densities, we find that $\text{Ba}_2\text{U}(\text{S}_2)_2\text{S}_2$ and $\text{Ba}_2\text{Th}(\text{S}_2)_2\text{S}_2$ display very similar distributions of the valence electrons. These are 6.7 , 7.3 , 8.4 , 9.8 , and 11.8 e[−] for S1, S2, Ba, Th, and U, respectively. Although some f electrons are present in $\text{Ba}_2\text{U}(\text{S}_2)_2\text{S}_2$, these have only a minor impact on the integrated charges per atom.

CONCLUSIONS

Two new ternary actinide sulfides, namely, $\text{Ba}_2\text{An}(\text{S}_2)_2\text{S}_2$ (An = U, Th), were synthesized at 1273 and 1173 K, respectively. Their structures were solved from single-crystal X-ray diffraction data. These isostructural compounds crystallize in the tetragonal space group $P4_2/nmc$ and adopt a new structure type that comprises Ba^{2+} cations and $[\text{An}(\text{S}_2)_2(\text{S}_2)_4]^{4-}$ layers. The An^{4+} cations in these layers are arranged linearly and are bridged by S^{2-} anions. This arrangement differs from those in other Ak/An/S compounds that contain S–S single bonds. Coordination about the An center, which has symmetry $4m2$, consists of two S_2^{2-} ions and four S^{2-} ions. This coordination may be described as pseudooctahedral if one considers the four S atoms and the centers of the two S–S pairs. The experimental optical direct band gap is $2.46(5)$ eV for $\text{Ba}_2\text{Th}(\text{S}_2)_2\text{S}_2$; this may be compared to the value of 2.2 eV from DFT calculations, performed with the HSE exchange–correlation potential, thus demonstrating the utility of applying this functional to 5f-electron systems. The calculated band gap of $\text{Ba}_2\text{U}(\text{S}_2)_2\text{S}_2$ is 1.8 eV.

■ ASSOCIATED CONTENT

5 Supporting Information

Crystallographic file in CIF format for $\text{Ba}_2\text{U}(\text{S}_2)_2\text{S}_2$ and $\text{Ba}_2\text{Th}(\text{S}_2)_2\text{S}_2$. This material is available free of charge via the Internet at <http://pubs.acs.org>.

■ AUTHOR INFORMATION

Corresponding Author

*E-mail: ibers@chem.northwestern.edu.

Notes

The authors declare no competing financial interest.

■ ACKNOWLEDGMENTS

The research was kindly supported at Northwestern University by the U.S. Department of Energy, Basic Energy Sciences, Chemical Sciences, Biosciences, and Geosciences Division and Division of Materials Science and Engineering (Grant ER-15522). Use was made of the IMSERC X-ray Facility at Northwestern University, supported by the International Institute of Nanotechnology. Funding for the optical studies was provided by National Science Foundation Grant CHE-1152547 and the NSF MRSEC (Grant DMR-1121262) at the Materials Research Center of Northwestern University.

■ REFERENCES

- (1) Manos, E.; Kanatzidis, M. G.; Ibers, J. A. In *The Chemistry of the Actinide and Transactinide Elements*, 4th ed.; Morss, L. R., Edelstein, N. M., Fuger, J., Eds.; Springer: Dordrecht, The Netherlands, 2010; Vol. 6, pp 4005–4078.
- (2) Bugaris, D. E.; Ibers, J. A. *Dalton Trans.* **2010**, *39*, 5949–5964.
- (3) Sunshine, S. A.; Kang, D.; Ibers, J. A. *J. Am. Chem. Soc.* **1987**, *109*, 6202–6204.
- (4) Narducci, A. A.; Ibers, J. A. *Inorg. Chem.* **1998**, *37*, 3798–3801.
- (5) Kwak, J.-e.; Gray, D. L.; Yun, H.; Ibers, J. A. *Acta Crystallogr., Sect. E: Struct. Rep. Online* **2006**, *62*, i86–i87.
- (6) Graham, J.; McTaggart, F. K. *Aust. J. Chem.* **1960**, *13*, 67–73.
- (7) Kohlmann, H.; Beck, H. P. Z. *Kristallogr.* **1999**, *214*, 341–345.
- (8) Noël, H. *J. Inorg. Nucl. Chem.* **1980**, *42*, 1715–1717.
- (9) Noël, H.; Potel, M. *Acta Crystallogr., Sect. B: Struct. Crystallogr. Cryst. Chem.* **1982**, *38*, 2444–2445.
- (10) Cody, J. A.; Ibers, J. A. *Inorg. Chem.* **1995**, *34*, 3165–3172.
- (11) Sutorik, A. C.; Kanatzidis, M. G. *J. Am. Chem. Soc.* **1991**, *113*, 7754–7755.
- (12) Cody, J. A.; Ibers, J. A. *Inorg. Chem.* **1996**, *35*, 3836–3838.
- (13) Choi, K.-S.; Patschke, R.; Billinge, S. J. L.; Waner, M. J.; Dantus, M.; Kanatzidis, M. G. *J. Am. Chem. Soc.* **1998**, *120*, 10706–10714.
- (14) Choi, K.-S.; Kanatzidis, M. G. *Chem. Mater.* **1999**, *11*, 2613–2618.
- (15) Wells, D. M.; Chan, G. H.; Ellis, D. E.; Ibers, J. A. *J. Solid State Chem.* **2010**, *183*, 285–290.
- (16) Brochu, R.; Padiou, J.; Grandjean, D. C. R. *Seances Acad. Sci., Ser. C* **1970**, *271*, 642–643.
- (17) Lelieveld, R.; Ijdo, D. J. W. *Acta Crystallogr., Sect. B: Struct. Crystallogr. Cryst. Chem.* **1980**, *36*, 2223–2226.
- (18) Brochu, R.; Padiou, J.; Prigent, J. C. R. *Acad. Sci. Paris* **1970**, *270*, 809–810.
- (19) Brochu, R.; Padiou, J.; Prigent, J. C. R. *Seances Acad. Sci., Ser. C* **1972**, *274*, 959–961.
- (20) Yao, J.; Ibers, J. A. *Z. Anorg. Allg. Chem.* **2008**, *634*, 1645–1647.
- (21) Bugaris, D. E.; Ibers, J. A. *Inorg. Chem.* **2012**, *51*, 661–666.
- (22) Bugaris, D. E.; Ibers, J. A. *J. Solid State Chem.* **2008**, *181*, 3189–3193.
- (23) Haneveld, A. J. K.; Jellinek, F. J. *Less-Common Met.* **1969**, *18*, 123–129.
- (24) APEX2, version 2009.5-1, and SAINT, *Data Collection and Processing Software*, version 7.34a; Bruker Analytical X-ray Instruments, Inc.: Madison, WI, USA, 2009.
- (25) SMART, *Data Collection*, version 5.054, and SAINT-Plus, *Data Processing Software for the SMART System* version 6.45a; Bruker Analytical X-ray Instruments, Inc.: Madison, WI, 2003.
- (26) Sheldrick, G. M. *Acta Crystallogr., Sect. A: Found. Crystallogr.* **2008**, *64*, 112–122.
- (27) Gelato, L. M.; Parthé, E. *J. Appl. Crystallogr.* **1987**, *20*, 139–143.
- (28) Spek, A. L. *PLATON, A Multipurpose Crystallographic Tool*; Utrecht University: Utrecht, The Netherlands, 2008.
- (29) Oh, G. N.; Ringe, E.; Van Duyne, R. P.; Ibers, J. A. *J. Solid State Chem.* **2012**, *185*, 124–129.
- (30) Koscielski, L. A.; Ringe, E.; Van Duyne, R. P.; Ellis, D. E.; Ibers, J. A. *Inorg. Chem.* **2012**, *51*, 8112–8118.
- (31) Amoretti, G.; Blaise, A.; Caciuffo, R.; Fournier, J. M.; Larroque, J.; Osborn, R. *J. Phys.: Condens. Matter* **1989**, *1*, 5711–5720.
- (32) Ballestracci, R.; Bertaut, E. F.; Pauthenet, R. *J. Phys. Chem. Solids* **1963**, *24*, 487–491.
- (33) Hohenberg, P.; Kohn, W. *Phys. Rev.* **1964**, *136*, 864–871.
- (34) Heyd, J.; Scuseria, G. E.; Ernzerhof, M. *J. Phys. Chem.* **2003**, *118*, 8207–8215.
- (35) Paier, J.; Marsman, M.; Hummer, K.; Kresse, G.; Gerber, I. C.; Angyan, J. G. *J. Chem. Phys.* **2006**, *125*, 249901–1–2.
- (36) Heyd, J.; Scuseria, G. E.; Ernzerhof, M. *J. Chem. Phys.* **2006**, *124*, 219906–1.
- (37) Perdew, J. P.; Burke, K.; Ernzerhof, M. *Phys. Rev. Lett.* **1996**, *77*, 3865–3868.
- (38) Henderson, T. M.; Paier, J.; Scuseria, G. E. *Phys. Status Solidi B* **2011**, *248*, 767–774.
- (39) Prodan, I. D.; Scuseria, G. E.; Martin, R. L. *Phys. Rev. B* **2007**, *76*, 033101-1–033101-4.
- (40) Hay, P. J.; Martin, R. L.; Uddin, J.; Scuseria, G. E. *J. Chem. Phys.* **2006**, *125*, 034712-1–034712-8.
- (41) Da Silva, J. L. F.; Ganduglia-Pirovano, M. V.; Sauer, J.; Bayer, V.; Kresse, G. *Phys. Rev. B* **2007**, *75*, 045121-1–045121-10.
- (42) Ganduglia-Pirovano, M. V.; Da Silva, J. L. F.; Sauer, J. *Phys. Rev. Lett.* **2009**, *102*, 026101-1–026101-4.
- (43) Kresse, G.; Furthmüller, J. *Comput. Mater. Sci.* **1996**, *6*, 15–50.
- (44) Kresse, G.; Joubert, D. *Phys. Rev. B* **1999**, *59*, 1758–1775.
- (45) Blöchl, P. E. *Phys. Rev. B* **1994**, *50*, 17953–17979.
- (46) Gajdos, M.; Hummer, K.; Kresse, G.; Furthmüller, J.; Bechstedt, F. *Phys. Rev. B* **2006**, *73*, 045112–1–9.
- (47) Hess, R. F.; Abney, K. D.; Burreis, J. L.; Hochheimer, H. D.; Dorhout, P. K. *Inorg. Chem.* **2001**, *40*, 2851–2859.
- (48) Selby, H. D.; Chan, B. C.; Hess, R. F.; Abney, K. D.; Dorhout, P. K. *Inorg. Chem.* **2005**, *44*, 6463–6469.
- (49) Rettig, S. J.; Trotter, J. *Acta Crystallogr., Sect. C: Cryst. Struct. Commun.* **1987**, *43*, 2260–2262.
- (50) Mizoguchi, H.; Gray, D.; Huang, F. Q.; Ibers, J. A. *Inorg. Chem.* **2006**, *45*, 3307–3311.
- (51) Bugaris, D. E.; Wells, D. M.; Yao, J.; Skanthakumar, S.; Haire, R. G.; Soderholm, L.; Ibers, J. A. *Inorg. Chem.* **2010**, *49*, 8381–8388.
- (52) Krönert, W.; Plieth, K. Z. *Anorg. Allg. Chem.* **1965**, *336*, 207–218.
- (53) Bader, R. F. W. *Atoms in molecules: a quantum theory*; International Series of Monographs on Chemistry 22; Oxford University Press, Inc.: New York, 1990.
- (54) Aubert, E.; Lebègue, S.; Marsman, M.; Thu Bui, T. T.; Jelsch, C.; Dahaoui, S.; Espinosa, E.; Angyán, J. G. *J. Phys. Chem.* **2011**, *A115*, 14484–14494.